Click Here for Full Article

Performance of soil moisture retrieval algorithms using multiangular L band brightness temperatures

M. Piles,[1] A. Camps,[1] M. Vall-llossera,[1] A. Monerris,[1] M. Talone,[1] and J. M. Sabater[2]

Received 24 August 2009; revised 11 January 2010; accepted 20 January 2010; published 9 June 2010.

[1] The Soil Moisture and Ocean Salinity (SMOS) mission of the European Space Agency was successfully launched in November 2009 to provide global surface soil moisture and sea surface salinity maps. The SMOS single payload is the Microwave Imaging Radiometer by Aperture Synthesis (MIRAS), an L band two-dimensional aperture synthesis interferometric radiometer with multiangular and polarimetric imaging capabilities. SMOS-derived soil moisture products are expected to have an accuracy of 0.04 m^3/m^3 over 50 × 50 km^2 and a revisit time of 3 days. Previous studies have remarked the necessity of combining SMOS brightness temperatures with auxiliary data to achieve the required accuracy. However, the required auxiliary data and optimal soil moisture retrieval setup need yet to be optimized. Also, the satellite operation mode (dual polarization or full polarimetric) is an open issue to be addressed during the commissioning phase activities. In this paper, an in-depth study of the different retrieval configurations and ancillary data needed for the retrieval of soil moisture from future SMOS observations is presented. A dedicated L2 Processor Simulator software has been developed to obtain soil moisture estimates from SMOS-like brightness temperatures generated using the SMOS End-to-End Performance Simulator (SEPS). Full-polarimetric brightness temperatures are generated in SEPS, and soil moisture retrievals are performed using vertical (T_{vv}) and horizontal (T_{hh}) brightness temperatures and using the first Stokes parameter (T_I). Results show the accuracy obtained with the different retrieval setups for four main surface conditions combining wet and dry soils with bare and vegetation-covered surfaces. Soil moisture retrievals using T_I exhibit a significantly better performance than using T_{hh} and T_{vv} in all scenarios, which indicates that the dual-polarization mode should not be disregarded. The uncertainty of the ancillary data used in the minimization process and its effect on the retrievals is thoroughly evaluated, and an optimum soil moisture retrieval configuration is devised.

Citation: Piles, M., A. Camps, M. Vall-llossera, A. Monerris, M. Talone, and J. M. Sabater (2010), Performance of soil moisture retrieval algorithms using multiangular L band brightness temperatures, *Water Resour. Res.*, *46*, W06506, doi:10.1029/2009WR008554.

1. Introduction

[2] Although soil only holds a small percentage of the total global water budget, soil moisture plays an important role in the Earth's water cycle; it is a key variable in the water and energy exchanges that occur at the land surface–atmosphere interface and conditions the evolution of weather and climate over continental regions. Global observations of the Earth's changing soil moisture are needed to enhance climate prediction skills and weather forecasting, which will benefit climate-sensitive socioeconomic activities, including water management, agricultural productivity estimation, and flood and drought hazards monitoring [*Entekhabi et al.*, 1999; *Krajewski et al.*, 2006; *Wagner et al.*, 2007]. Despite being a critical state variable of the Earth system, its high spatial and temporal variability makes soil moisture a difficult parameter to measure, and there are no current observing systems to monitor it globally. Nevertheless, in the last decades, several studies have remarked the potential of using L band microwave remote sensing to monitor soil moisture [*Njoku and Entekhabi*, 1996; *Schmugge et al.*, 2002], and two space missions have been proposed to globally measure soil moisture using this technology: the European Space Agency (ESA) launched the Soil Moisture and Ocean Salinity (SMOS) satellite mission in November 2009 [*Kerr et al.*, 2001], and NASA will launch the Soil Moisture Active Passive (SMAP) satellite mission in 2014 [*National Research Council*, 2007].

[3] The SMOS mission aims at providing the first global measurements of the Earth's surface soil moisture with an accuracy of 0.04 m^3/m^3 over 50 × 50 km^2 and a temporal resolution of 3 days. There is also a high interest in obtaining vegetation water content maps with an accuracy of 0.2 kg/m^2 from future SMOS observations [*European Space*

[1] Remote Sensing Laboratory, Departament de Teoria del Senyal i Comunicacions, Universitat Politècnica de Catalunya, IEEC, CRAE-UPC, SMOS Barcelona Expert Centre, Barcelona, Spain.

[2] European Centre for Medium-Range Weather Forecasts, Reading, UK.

Copyright 2010 by the American Geophysical Union.
0043-1397/10/2009WR008554

Agency, 2003]. The SMOS payload is a totally new type of instrument, the Microwave Imaging Radiometer by Aperture Synthesis (MIRAS), that provides two-dimensional brightness temperature (T_B) measurements of the Earth at different incidence angles with a ground resolution varying between 30 and 100 km, depending on the position on the field of view [*Martín-Neira et al.*, 2002]. MIRAS can work in two operation modes: the dual-polarization and the full-polarimetric modes. In dual-polarization mode, MIRAS measures the T_B values in horizontal and vertical polarizations, whereas in full-polarimetric mode, MIRAS measures the four Stokes parameters (see Appendix A).

[4] The theory behind L band microwave remote sensing of soil moisture is based on the large contrast between the dielectric constants of dry soil (~4) and water (~80) [*Jackson and Schmugge*, 1989; *Ulaby et al.*, 1981]. The dielectric constant of soils is highly related to the soil moisture content s_m and depends on the soil type [*Wang and Schmugge*, 1980; *Dobson et al.*, 1985]. In addition to the soil dielectric constant, other soil and vegetation parameters are known to play a significant role in the L band microwave emission and therefore must be accounted for in the retrieval process, namely, surface temperature T_s, surface soil roughness (determined using the soil roughness parameter h_s), vegetation albedo ω, and vegetation optical depth τ (from which vegetation water content maps can be derived [*van de Griend and Wigneron*, 2004]). Several configurations have been proposed for decoupling the contribution of each of these surface parameters and hence retrieving soil moisture from SMOS observations. For instance, *Wigneron et al.* [1995] presented the possibility of simultaneously retrieving s_m and τ (the two-parameter (2-P) retrieval method) using experimental L band observations over crop fields. The so-called 3-P retrieval method, in which T_s is retrieved in addition to s_m and τ, is applied to a synthetic simulated data set as given by *Pellarin et al.* [2003]. By extension, the N-P retrieval method, where N corresponds to the number of parameters that are retrieved, is analyzed by *Pardé et al.* [2004] and *Camps et al.* [2005]. In all these studies, the parameters are retrieved by minimizing a cost function which accounts for the weighted squared differences between measured and simulated brightness temperatures, using for the latter the $\tau - \omega$ radiative model [*Ulaby and Wilson*, 1985; *Mo et al.*, 1982], and between the retrieved quantities and their estimated values, with weights reflecting a priori uncertainties on these variables.

[5] Since different retrieval setups lead to different accuracy results, an in-depth study of the different cost function configurations for retrieving soil moisture estimates from future SMOS observations is paramount. Although some retrieval issues regarding the parameters to be retrieved have been analyzed in the above-cited studies, the a priori information used in the retrievals and its required uncertainty are key aspects yet to be determined. Also, the optimum MIRAS operation mode (dual polarization or full polarimetric) is still an open issue. In the present study, the performance of different retrieval configurations, depending on the a priori information that is used in the retrievals and its associated uncertainty, is analyzed using SMOS-like T_B values generated by the SMOS End-to-End Performance Simulator (SEPS) [*European Space Agency*, 2006]. To obtain soil moisture from SEPS realistic T_B, this study uses the L2 Processor Simulator. The L2 Processor Simulator is a dedicated software developed from the experience gained in previous works on SMOS-derived salinity studies [*Talone et al.*, 2009; *Sabia et al.*, 2010] and land field experiments at L band [*Monerris*, 2009]; it is a simplified version of the ESA's SMOS Level 2 Processor, which integrates the forward model and optimization algorithm described in section 2, and is designed to be used with SEPS output data. Hence, the parameters dominating the microwave emission at L band (s_m, h_s, T_s, ω, and τ) have been considered as possible a priori information to be used in the retrievals, and the uncertainties of s_m and h_s over bare soil scenarios and of ω and τ over vegetation-covered scenarios have been tuned from very large values to very restrictive conditions in different L2 Processor simulations. Note that T_s is assumed to be known from thermal infrared remote sensing with an accuracy of 2 K [*Wan*, 2008]. Setting this rather strong constraint on T_s has been shown to be preferable in previous L band retrieval studies [*Pellarin et al.*, 2003; *Pardé et al.*, 2004; *Davenport et al.*, 2005]. Then, when all uncertainties are set to large values, all parameters are free and retrieved (i.e., an N-P approach). In contrast, when a high constraint is imposed on a parameter, it is set to a constant value, and therefore, it is not retrieved (i.e., 2-P is explored when a high constraint is imposed on h_s and ω and s_m and τ are free and retrieved). Also, parameters are retrieved using vertical (T_{vv}) and horizontal (T_{hh}) polarizations separately and using the first Stokes parameter (T_I), which may be linked to the choice of the full-polarimetric mode or the dual-polarization mode, respectively. From these simulations, the uncertainty of the ancillary data used in the minimization process and its impact on the retrieval of soil moisture and vegetation optical depth from SMOS-like observations is thoroughly evaluated, the use of the two polarizations separately and of the first Stokes parameter are explored, and an optimal retrieval configuration is devised.

2. Soil Moisture Retrieval

[6] Soil moisture retrieval consists of inverting a geophysical model function by finding the set of input variables (soil moisture and other model parameters such as soil temperature, soil roughness, vegetation albedo, and vegetation opacity) which generate the brightness temperatures that best match the "observed" brightness temperatures. The geophysical model function used in this study to mimic the Earth emission at L band, the so-called forward model, is described in section 2.1. In the case of SMOS, auxiliary data must be combined with SMOS-like modeled brightness temperatures on a cost function which must be well defined and adequately minimized to retrieve soil moisture fulfilling the mission requirements. The simulation strategy and the optimization scheme used in this paper to devise an optimal soil moisture retrieval configuration from SMOS data are fully described and analyzed in section 2.2.

2.1. Forward Model

[7] The bare soil emissivity depends on its surface roughness (determined using the soil roughness parameter h_s), temperature T_s, and soil dielectric constant, which is in turn related to the soil moisture content s_m and soil type [*Choudhury et al.*, 1979]. When the soil is covered by vegetation, its emission is affected by the canopy layer: it attenuates the soil emission and adds its own contribution.

Table 1. Selected Values of Soil Moisture, Soil Roughness Parameter, Soil Temperature, Vegetation Opacity, and Vegetation Albedo for the Four Master Scenarios[a]

	s_m (m^3/m^3)	h_s	T_s (K)	τ (Np)	ω
Bare dry soil	0.02	0.2	300	0	0
Bare wet soil	0.2	0.2	300	0	0
Dry soil plus canopy	0.02	0.2	300	0.24	0
Wet soil plus canopy	0.2	0.2	300	0.24	0

[a]Here s_m, soil moisture; h_s, soil roughness parameter; T_s, soil temperature; τ, vegetation opacity; ω, vegetation albedo.

In this study, the well-known $\tau - \omega$ radiative transfer model has been used to model the forward brightness temperatures at L band [*Mo et al.*, 1982; *Ulaby and Wilson*, 1985]. This model is based on two vegetation parameters, the optical depth or opacity τ, which accounts for the attenuation, and the single-scattering albedo ω, which accounts for dispersion of the radiation within the vegetation:

$$T_{pp} = (1-\omega)(1-\gamma)(1+\Gamma_S\gamma)T_V + (1-\Gamma_S)T_S\gamma, \quad (1)$$

where T_{pp} ($p = h$ for the horizontal polarization and $p = v$ for the vertical polarization) are the modeled brightness temperatures, $\Gamma_S(\theta, p)$ is the soil reflectivity, $\gamma(\theta, p)$ is the transmissivity of the vegetation layer, T_S is the effective soil temperature, and T_V is the effective temperature of the vegetation.

[8] The soil reflectivity $\Gamma_S(\theta, p)$ depends on incidence angle θ and polarization p and can be expressed as

$$\Gamma_S(\theta,p) = \left[(1-Q)\Gamma_S^*(\theta,p) + Q\Gamma_S^*(\theta,p)\right]\exp[-h_s\cos^n(\theta)] \quad (2)$$

where $\Gamma_S^*(\theta, p)$ is the power reflection coefficient of the flat soil (squared amplitude of the Fresnel reflection coefficient) that depends on the soil moisture through the dielectric constant [*Wang and Schmugge*, 1980], Q is the polarization mixing factor, n expresses the angular dependence of roughness, and h_s is the soil roughness parameter [*Wang and Choudhury*, 1981].

[9] The transmissivity of the vegetation layer $\gamma(\theta, p)$ can be expressed as a function of the vegetation optical thickness τ and the incidence angle θ:

$$\gamma(\theta,p) = \exp[-\tau/\cos(\theta)]. \quad (3)$$

[10] The vegetation optical depth can be linearly related to the vegetation water content (VWC) (kg/m^2) through an empirical parameter b [*van de Griend and Wigneron*, 2004]:

$$\tau = b(\mathrm{VWC}). \quad (4)$$

[11] A detailed analysis of the soil roughness effects performed by *Wigneron et al.* [2001] showed that both Q and n could be set equal to zero at L band and that the roughness parameter h_s could be semiempirically estimated, comprising most surface roughness conditions. This approach has been followed in this study, where h_s is set constant and equal to 0.2, representing rather smooth roughness conditions. This is consistent with L band airborne and ground-based experiments, where soil roughness was generally found to be rather smooth over agricultural or natural areas [*Jackson et al.*, 1999; *Wigneron et al.*, 2007]. Also, recent studies have observed a dependence of h_s on soil moisture content [*Wigneron et al.*, 2001; *Schneeberger et al.*, 2004; *Escorihuela et al.*, 2007]. However, these studies are performed under very local conditions, yet there is no evidence of the potential benefits that they may be introduced at global scale. To date, the accuracy of the previous approaches linking h_s and soil moisture is not well established for a variety of roughness conditions, and the relationship between h_s, surface roughness characteristics, and soil moisture has not been fully understood. Thus, in the present study, h_s is retrieved as a free parameter, without using any dependency on soil moisture or surface roughness characteristics.

[12] There is some experimental evidence indicating possible polarization dependence of both τ and ω. However, this dependence has been observed mainly during field experiments over vegetation elements that exhibit a clear uniform orientation, such as vertical stalks in tall grasses, grains, and maize [*Kirdiashev et al.*, 1979; *Wigneron et al.*, 1995; *Hornbuckle et al.*, 2003], whereas canopy and stem structure of most vegetation covers are randomly oriented. Furthermore, the effects of any systematic orientation of vegetation elements would most likely be minimized at satellite scales [*Owe et al.*, 2001]. Hence, (1) has been simplified assuming that τ and ω are polarization- and angle-independent. Also, it is assumed that the temperature of the vegetation canopy is in equilibrium with the soil temperature ($T_S = T_V = T_s$), since at SMOS overpass times (6 A.M. and 6 P.M.) temperature gradients within the soil and vegetation should be minimized [*Hornbuckle and England*, 2005].

[13] Four master scenarios (bare dry soil, bare wet soil, vegetation-covered dry soil, and vegetation-covered wet soil) have been created using SEPS with the aim of comparing the different retrieval configurations and addressing separately the contribution of the bare soil parameters (s_m, T_s, and h_s) and of the vegetation descriptors (τ and ω) on a dry and on a wet soil. Constant input parameters have been used in the simulations to evidence the contribution of each parameter in the final result and to facilitate the analysis. Soil moisture values of 0.02 m^3/m^3 and 0.2 m^3/m^3 have been defined to represent dry and wet soils, respectively; the roughness parameter h_s is set to 0.2; and nominal values are given to the vegetation parameters τ = 0.24 Np and ω = 0 [*European Space Agency*, 2007]. These parameters have been summarized in Table 1.

2.2. Optimization Scheme

[14] SMOS-like full-polarimetric brightness temperatures have been simulated over land for the four master scenarios in Table 1 using SEPS [*European Space Agency*, 2006]. Next, these data have been used as input to the L2 Processor Simulator, where surface parameters have been retrieved by minimizing a cost function (CF), using the generalized least squares iterative algorithm of Levenberg-Marquardt [*Marquardt*, 1963]. The dedicated L2 processor has been developed to be used with SEPS output data, in preparation for the upcoming SMOS data, and with a structure as similar as possible to the ESA's SMOS Level 2 Processor [*European Space Agency*, 2007], so that the results obtained

could be potentially applicable to real SMOS data. Hence, assuming that the measurement errors are Gaussian, the cost function for observation model misfits can be expressed as

$$\mathrm{CF} = \sum_{n=1}^{N} \frac{\| \overline{F}_n^{\mathrm{meas}} - \overline{F}_n^{\mathrm{model}} \|^2}{\sigma_{F_n}^2} + \sum_{i=1}^{M} \frac{(p_i - p_{i0})^2}{\sigma_{p_{i0}}^2}, \qquad (5)$$

where $\overline{F}^{\mathrm{meas}}$ and $\overline{F}^{\mathrm{model}}$ are vectors of length N containing the brightness temperatures at different incidence angles, measured by MIRAS and obtained using the forward models, respectively. N is the number of observations of the same point in a satellite overpass; σ_{F_n} is the radiometric accuracy for the nth observation; p_i (i = 1, …, M) are the retrieved physical parameters that may influence the modeled T_B, including s_m, T_s, h_s, τ, and ω; p_{i0} are prior estimates of parameters p_i (obtained from other sources such as satellite measurements or model outputs, the auxiliary information); and σ_{pi0} is the uncertainty on the a priori parameter p_{i0}. The value of σ_{pi0} is used to parameterize the constraint on the parameter p_i in the retrievals: p_i can be set to be free (σ_{pi0} = 100; no a priori information is used), it can be constrained to be more or less close to the reference value p_{i0}, or it can be constant ($\sigma_{pi0} < 10^{-3}$, assuming high accuracy on the a priori information). Note that p_{i0} are specified mph a priori, whereas p_i values are adjusted during the minimization process.

[15] The retrieval of the geophysical parameters can be formulated using the vertical (vv) and horizontal (hh) polarizations separately ($\overline{F}_n = [T_{vv}, T_{hh}]^T$ in the Earth reference frame and $\overline{F}_n = [T_{xx}, T_{yy}]^T$ in the antenna frame), or using the first Stokes parameter ($\overline{F}_n = [T_I]^T = [T_{xx} + T_{yy}]^T = [T_{hh} + T_{vv}]^T$) (Appendix A). These two approaches have been considered in this study. If retrievals are formulated using the two polarizations separately, the Faraday rotation in the ionosphere should be corrected since at L band it can be sufficient so as to cause errors in the retrieval of the surface parameters [*Vine and Abraham*, 2002]. Therefore, as third and/or fourth Stokes parameters could be highly useful for a precise Faraday correction, the CF formulation in the Earth or antenna frame is usually linked to the use of the full-polarimetric mode. Also, large singularities are induced by the inversion of the geometric and Faraday rotations while passing the measured brightness temperatures from antenna to Earth frame in dual-polarization mode [*Waldteufel and Caudal*, 2002]. In contrast, T_I is unaffected by Faraday rotation; retrievals using the first Stokes parameter can be calculated in the two operation modes, with the difference that when the dual-polarization mode is used, the integration time is maximized and better radiometric sensitivity could be obtained [*Camps et al.*, 2005].

[16] In this study, the impact that the uncertainty of the ancillary data used in the minimization process has on the retrieval of soil moisture and vegetation optical depth from SMOS-like observations has been evaluated. To do so, the uncertainties of s_m and h_s over the bare soil scenarios and of τ and ω over the vegetation-covered scenarios have been progressively tuned in different L2 Processor simulations, starting from very large values (no prior information is added) to very restrictive conditions (high confidence on the a priori information). T_s is set to its first-guess value during the retrieval process with an accuracy of 2 K, in agreement with results of previous studies [*Pellarin et al.*, 2003; *Pardé et al.*, 2004; *Davenport et al.*, 2005]. Also, each simulation has been formulated using (T_{vv}, T_{hh}) and using T_I so as to compare these two approaches. Note that, to date, the formulation of the SMOS-derived soil moisture retrieval problem on the Earth reference frame (and therefore the use of the full-polarimeric mode) is the preferred one [*Pardé et al.*, 2004; *Saleh et al.*, 2009]. Hence, we present the formulation of the problem in terms of T_I as an alternative approach, since retrievals using the first Stokes parameter could provide the benefit of having less angular dependency than (T_{vv}, T_{hh}), therefore, reducing the degrees of freedom during the inversion process, which could lead to better soil moisture retrievals. Also, retrievals using T_I are more robust to geometric and Faraday rotations, which is critical from an operational point of view.

[17] It is important to outline that retrievals are performed under the following guidelines and assumptions.

[18] 1. The geophysical models used in the L2 Processor Simulator are the same as in SEPS. Then, the effect of the model used is not affecting the results.

[19] 2. The performance of the cost function configuration is not dependent on σ_{F_n}, since the absolute accuracy of the radiometric measurements is available on the SEPS output and is used in the retrievals.

[20] 3. The search limits of the retrieved variables in the CF have been reduced within reasonable bounds, namely, $0 \le s_m \le 0.4$ m^3/m^3, $250 \le T_s \le 350$ K, $0 \le h_s \le 5$, $0 \le \tau \le 3$ Np, and $0 \le \omega \le 0.3$, to reduce the computational time.

[21] 4. The reference values of the parameters used in the CF are determined from a normal distribution with a standard deviation of 2 K for T_s, 0.05 for h_s, 0.1 for ω, 0.1 Np for τ, and 0.04 m^3/m^3 for s_m, added to the original values. Thus, since realistic initial values are used in the minimization process, the study focuses on selecting the optimum level of a priori information to be used in the retrievals and its associated uncertainty.

[22] These simplifications are needed to make a homogeneous and approachable intercomparison study of the different retrieval configurations. However, note that further studies will be required to assess the limitations imposed by heterogeneity of vegetation cover and soil characteristics within a satellite footprint.

3. Simulation Results

[23] In the first stage, a bare soil scenario is simulated to retrieve s_m, T_s, and h_s. It is assumed that T_s is known by means of thermal infrared observations and/or meteorological models with an accuracy of 2 K, so σ_{T_s} is set to 2 K [*Wan*, 2008]. The entire range of variability of s_m and h_s on the CF is analyzed, and results are shown for bare dry and wet soil in Figures 1a and 1b, respectively, using (T_{hh}, T_{vv}) and in Figures 2a and 2b, respectively, using T_I. From these results, it can be inferred that it is important, although not critical, to add a restriction on the soil roughness parameter h_s. An expected error of 0.05 on h_s is therefore suggested for the soil moisture retrieval scheme. With this constraint, SMOS scientific requirements are met in the case of using T_I (a s_m root-mean-square error (RMSE) of 0.02 m^3/m^3 is obtained over dry soils and of 0.04 m^3/m^3 over wet soils). In the case of using (T_{hh}, T_{vv}), however, a s_m RMSE of ≈0.08–0.09 m^3/m^3 is obtained over both dry and wet soils.

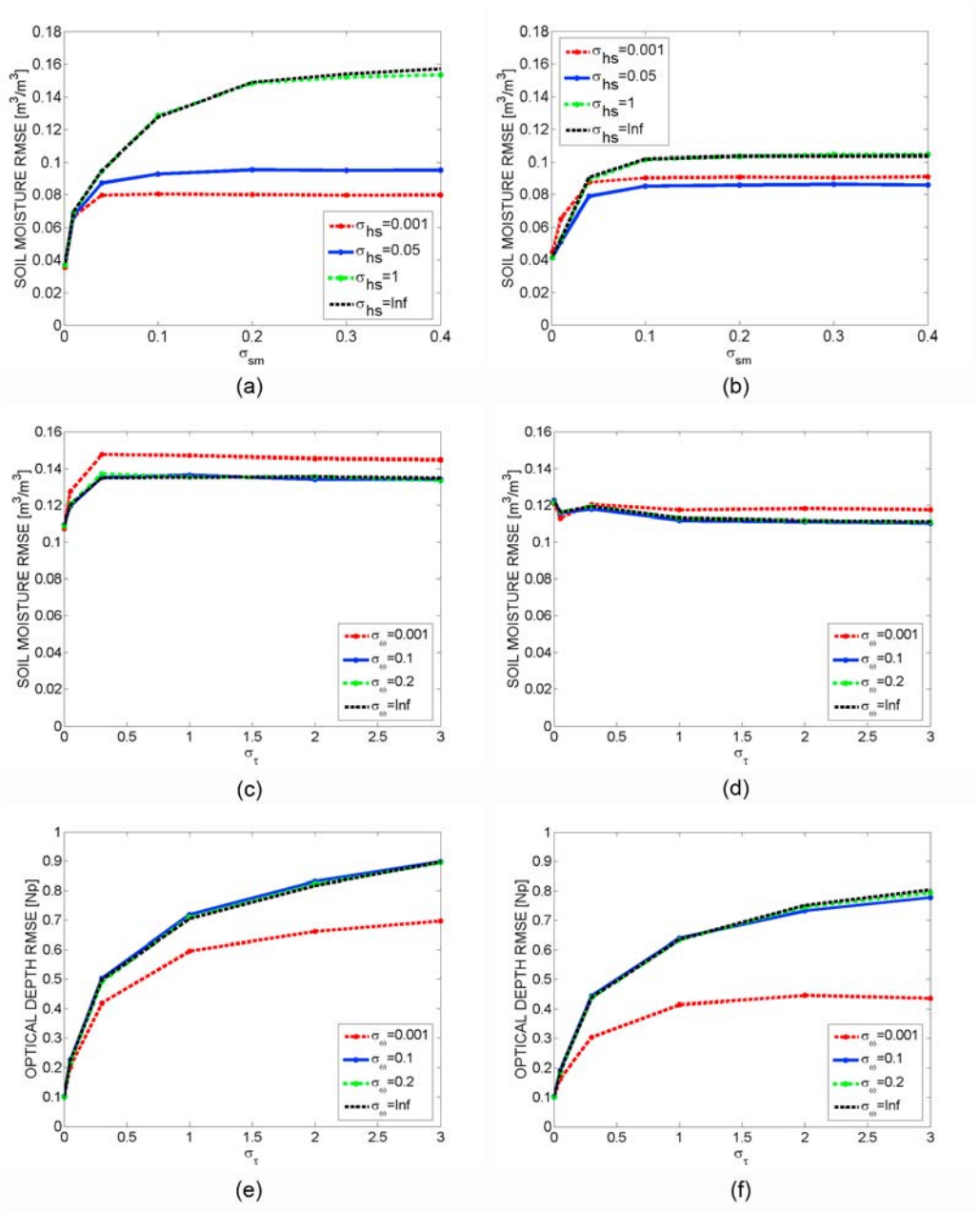

Figure 1. Graphical plots of retrievals formulated using vertical (T_{vv}) and horizontal (T_{hh}) polarizations. Retrieved soil moisture RMSE over a (a) bare dry soil and (b) bare wet soil scenario, for different uncertainties on auxiliary soil moisture (σ_{s_m}) and roughness parameter (σ_{h_s}). Retrieved optical depth RMSE over a (c) vegetation-covered dry soil, (d) vegetation-covered wet soil, (e) vegetation-covered dry soil, and (f) vegetation-covered wet soil scenario, for different uncertainties on auxiliary optical depth (σ_τ) and albedo (σ_ω).

[24] After this initial study, a vegetation-covered scenario is simulated to retrieve s_m, T_s, τ, and ω. On these experiments h_s is set to 0.2 and will not be retrieved so as to decouple the effect of soil roughness, and no restrictions are added on soil moisture (σ_{s_m} = 100 m^3/m^3). Therefore, the simulations over vegetation-covered scenes embrace the entire range of variability of the vegetation descriptors τ and ω, keeping σ_{s_m} = 100 m^3/m^3 and σ_{T_s} = 2 K. Retrieved s_m RMSE versus the uncertainty on s_m is shown for dry and wet soils in Figures 1a and 1b, respectively, using (T_{hh}, T_{vv}), and in Figures 2a and 2b using T_I. From Figures 1c, 1d, 2c, and 2d, it can be noted that there is a strong decrease of the brightness temperature sensitivity to s_m in the presence of vegetation and that s_m RMSE increases with σ_τ. When $\sigma_\tau \rightarrow \infty$, s_m RMSE converges nearly to the same values in the two formulations (s_m RMSE $\approx$ 0.11–0.14 m^3/m^3 for vegetation-covered dry soils and s_m RMSE $\approx$ 0.10–0.11 m^3/m^3 for vegetation-covered wet soils). Since there is also a high interest in deriving VWC maps from future SMOS observations, the optical depth RMSE obtained with the different simulations has also been analyzed and is plotted versus the uncertainty on τ in Figures 1e and 1f for

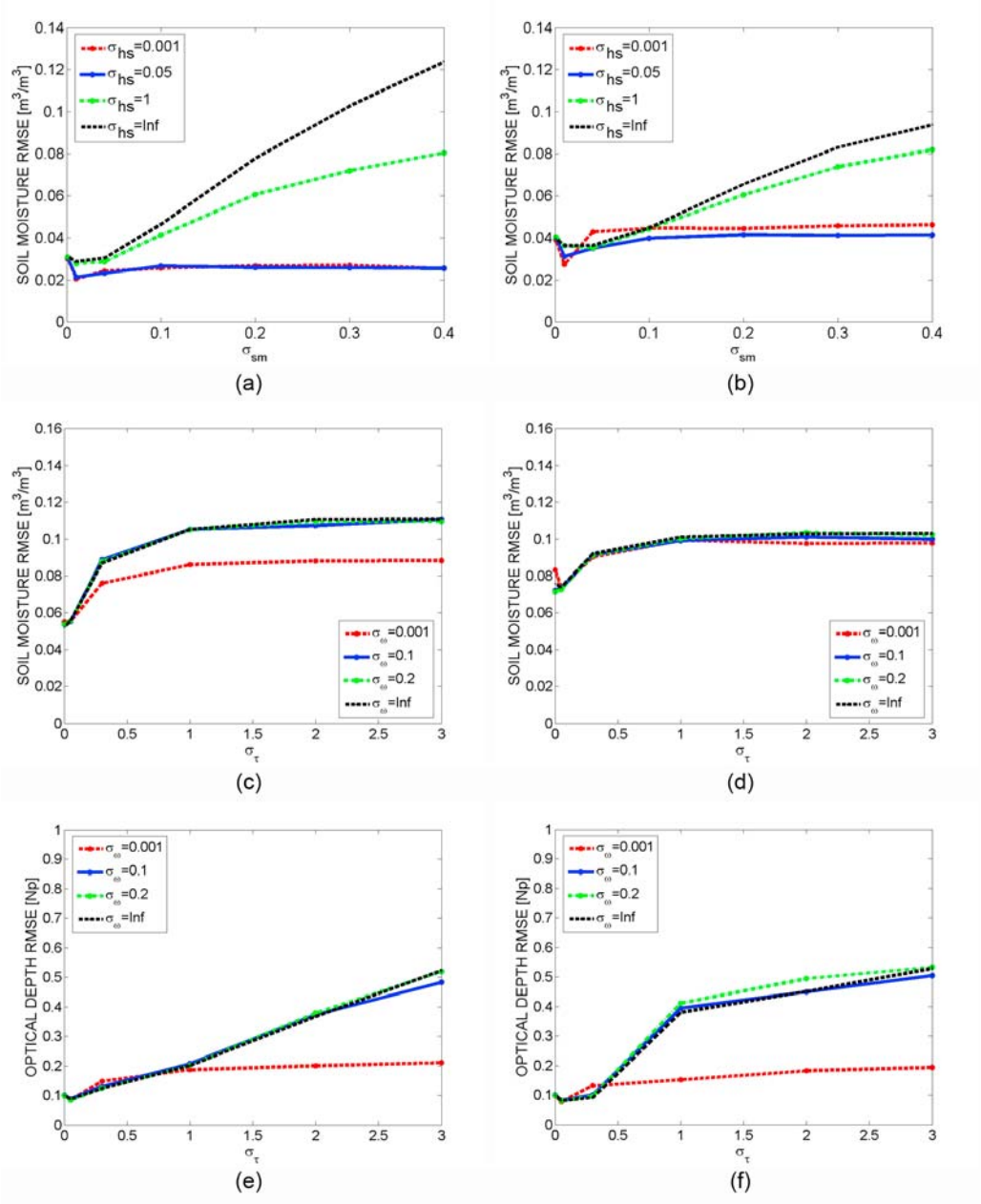

Figure 2. Graphical plots of retrievals formulated using the first Stokes parameter (T_I). Retrieved soil moisture RMSE over a (a) bare dry soil and (b) bare wet soil scenario, for different uncertainties on auxiliary soil moisture (σ_{s_m}) and roughness parameter (σ_{h_s}). Retrieved optical depth RMSE over a (c) vegetation-covered dry soil, (d) vegetation-covered wet soil, (e) vegetation-covered dry soil, and (f) vegetation-covered wet soil scenario, for different uncertainties on auxiliary optical depth (σ_τ) and albedo (σ_ω).

vegetation-covered dry and wet soils, respectively, using (T_{hh}, T_{vv}) and in Figures 2e and 2f, respectively, using T_I. From Figures 1e, 1f, 2e, and 2f, it can be remarked that optical depth RMSE increases monotonically with σ_τ when using the two formulations. In the case of high uncertainty on the vegetation parameters ($\sigma_\tau = 3$, $\sigma_\omega \rightarrow \infty$), τ RMSE converges to the same values for dry and wet soils: $\tau \approx 0.8$–0.9 Np using (T_{hh}, T_{vv}) and $\tau \approx 0.5$ Np using T_I.

[25] The most beneficial retrieval configuration will be the one providing the minimum s_m and τ RMSE. The choice of σ_τ is clear: since s_m and τ RMSE increase monotonically with σ_τ, the ideal case would be to fix it ($\sigma_\tau = 0.001$ Np). Yet, although the study is theoretical and covers all the range of variability of the parameters, only realistic uncertainties in the ancillary data must be considered in selecting the optimum. Thus, considering the auxiliary sources available, an expected error of 0.1 Np in vegetation optical depth is suggested in the CF formulation.

[26] Regarding the choice of σ_ω, a clear improvement can be observed on τ RMSE when a high constraint is imposed

on ω ($\sigma_\omega = 0.001$) and $\sigma_\tau > 0.3$ Np, whereas a lower constraint of 0.1 seems to have little or no effect (compared to the case of no restrictions on ω, $\sigma_\omega \rightarrow \infty$); adding or no restrictions on ω, though, does not cause s_m RMSE to vary significantly. From these results, it can be inferred that no constraints on ω are needed under nominal vegetation conditions. Note that auxiliary information for ω could be needed in the case of heterogeneous areas and dense vegetation covers [*Pardé et al.*, 2004; *Davenport et al.*, 2005]. With these constraints ($\sigma_\tau = 0.1$ Np, $\sigma_\omega \rightarrow \infty$), a s_m RMSE of 0.11 m^3/m^3 is obtained in vegetation-covered scenarios using (T_{hh}, T_{vv}), and a s_m RMSE of ≈0.06–0.07 m^3/m^3 is obtained using T_I. These results indicate that the s_m RMSE mission requirement of 0.04 m^3/m^3, which is also the accuracy of most soil moisture sensors (Delta-T Devices Ltd., Thetaprobe soil moisture sensors specifications, 2007, http://www.delta-t.co.uk/products.html), could not be fully satisfied in the presence of vegetation.

[27] Regarding τ retrievals, adding the suggested restrictions on the CF of $\sigma_\tau = 0.1$ Np and $\sigma_\omega = 0.1$ is notably improving the accuracy of the results (a τ RMSE of 0.2 Np is obtained using (T_{hh}, T_{vv}) and of 0.1 Np using T_I).

[28] From (4), the optical depth can be linearly related to the VWC using the so-called b parameter, which depends mainly on crop type and frequency. At L band, a value of b = 0.15 m^2/kg was found to be representative of most agricultural crops at L band, with the exception of grasses [*van de Griend and Wigneron*, 2004]. Using this value, VWC maps with an accuracy of ≈3.3–6 kg/m^2 could be obtained in the case of complete uncertainty on the vegetation parameters ($\sigma_\tau = 3$ Np, $\sigma_\omega \rightarrow \infty$), and VWC maps with an accuracy of ≈0.6–1.3 kg/m^2 could be obtained in the case of adding the suggested τ and ω restrictions. These calculations, although not precise, indicate that the use of vegetation optical depth data as auxiliary information in the minimization process is critical to derive VWC maps from SMOS at the required accuracy of 0.2 kg/m^2.

4. Conclusions

[29] This study has analyzed the impact in the soil moisture retrieval performance of adding ancillary data with different associated uncertainty and of using vertical (T_{vv}) and horizontal (T_{hh}) polarizations separately or the first Stokes parameter (T_I), which may be linked to the choice of the full-polarimetric or dual-polarization SMOS operation mode. Following the optimization scheme described in section 2.2, the performance of the different methods has been analyzed and presented in terms of retrieved soil moisture RMSE and retrieved optical depth RMSE over four master homogeneous scenarios: (1) bare dry soil, (2) bare wet soil, (3) vegetated dry soil, and (4) vegetated wet soil. The main conclusions can be summarized as follows.

[30] 1. Over bare soils, this study shows that adding ancillary information on soil roughness (h_s) to the cost function considerably improves the accuracy of s_m retrievals. It is in good agreement with other L band retrieval studies [*Pardé et al.*, 2004; *Davenport et al.*, 2005]. With the suggested uncertainty of 0.05 on ancillary h_s data, and of 2 K on T_s data (σ_{T_S} = 2K, from thermal infrared observations or meteorological models), SMOS science requirements could be met in the case of using T_I (s_m RMSE of 0.02 m^3/m^3 and 0.04 m^3/m^3 are obtained over dry and wet soils, respectively). Using (T_{hh}, T_{vv}), however, a s_m RMSE of ≈0.08–0.09 m^3/m^3 is obtained over both dry and wet soils.

[31] 2. As expected, there is a strong decrease of the brightness temperature sensitivity to s_m in the presence of vegetation. Results indicate that adding vegetation albedo does not cause s_m and τ retrievals to vary significantly, and $\sigma_\omega \rightarrow \infty$ is proposed. Note that ω information is not needed in the particular nominal vegetation case studied (τ = 0.24 Np and $\omega = 0$) but could be needed in the general case of heterogeneous areas and dense vegetation covers [*Pardé et al.*, 2004; *Davenport et al.*, 2005]. In contrast, the uncertainty on the auxiliary optical depth data used in the CF is highly affecting s_m retrievals; s_m RMSE increases with σ_τ, converging to ≈0.11–0.14 m^3/m^3 for vegetation-covered dry soil and ≈0.10–0.11 m^3/m^3 for wet soil, when $\sigma_\tau \rightarrow \infty$. From these results, and considering the auxiliary sources available, a constraint of $\sigma_\tau = 0.1$ Np in the CF is recommended. With this constraint, a s_m RMSE of 0.11 m^3/m^3 is obtained in vegetation-covered scenarios using (T_{hh}, T_{vv}) and of ≈0.06–0.07 m^3/m^3 using T_I.

[32] 3. The use of τ ancillary information on the CF is critical to obtain VWC maps from τ retrievals with an accuracy of 0.2 kg/m^2; retrieved τ RMSE increases monotonically with the uncertainty of the τ ancillary information (σ_τ) used for the CF, converging to ≈0.8–0.9 Np using (T_{hh}, T_{vv}) and to ≈0.5 Np using T_I, in the case of high uncertainty on the vegetation parameters ($\sigma_\tau = 3$ Np, $\sigma_\omega \rightarrow \infty$). With the suggested τ and ω constraints ($\sigma_\tau = 0.1$, $\sigma_\omega \rightarrow \infty$), a τ RMSE of 0.2 Np is obtained using (T_{hh}, T_{vv}) and of 0.1 Np using T_I. The τ retrievals in a previous overpass could be used as auxiliary information in retrievals at time t, as given by *Wigneron et al.* [2000] and *Pardé et al.* [2004]. If no τ auxiliary information is available, an alternative approach is presented by *Meesters et al.* [2005], where τ is retrieved from passive observations at 6.6 GHz using only land surface temperature as ancillary information.

[33] 4. Soil moisture and vegetation optical depth retrievals show a better performance if the minimization is formulated using the Stokes parameter T_I than using the Earth reference frame (T_{hh}, T_{vv}). This result suggests that the dual-polarization mode should not be discarded a priori, since T_I should have better radiometric sensitivity in the dual-polarization mode than in full-polarimetric mode. In addition, retrievals using T_I are more robust to geometric and Faraday rotations than (T_{hh}, T_{vv}). Note that this effect has been perfectly corrected in the simulations but can be critical from an operational point of view.

[34] 5. It must be remarked that if a priori information on the land surface conditions can be available, restrictions on h_s, T_s, and τ are highly recommended. The better the accuracy of these auxiliary sources, the better are the s_m and τ retrievals that could be obtained. All things considered, the required uncertainty levels for auxiliary input data are $\sigma_{h_s} = 0.05$, $\sigma_{T_s} = 2$ K, and $\sigma_\tau = 0.1$ Np.

[35] The results presented in this paper can help to define the SMOS operation mode, which will be decided during the commissioning phase, and to define the soil moisture retrieval scheme and the auxiliary data needed in the operational SMOS Level 2 Processor. These are crucial issues that have to be addressed to retrieve accurate global soil moisture estimates from SMOS, which are expected to lead to better water resource management and will further our knowledge of the continuous exchange of water between the

oceans, the land, and the atmosphere in the Earth's water cycle.

Appendix A: Stokes Parameters

[36] The polarization of an electromagnetic wave can be completely described by the four Stokes parameters I, Q, U, and V. The first Stokes parameter (I) describes the total intensity of electromagnetic emission, and the second Stokes parameter (Q) is the difference between the intensity in two orthogonal directions in a given polarization frame, e.g., vertical and horizontal polarizations. The third (U) and fourth (V) Stokes parameters represent the real and imaginary parts of the cross correlation between these orthogonal polarizations, respectively [*Randa et al.*, 2008]:

$$\begin{aligned} I &= \frac{\left\langle |E_v|^2 \right\rangle + \left\langle |E_h|^2 \right\rangle}{\eta}, \\ Q &= \frac{\left\langle |E_v|^2 \right\rangle - \left\langle |E_h|^2 \right\rangle}{\eta}, \\ U &= \frac{2Re\langle E_v E_h^* \rangle}{\eta}, \\ V &= \frac{2\mathrm{Im}\langle E_v E_h^* \rangle}{\eta}. \end{aligned} \tag{A1}$$

E_v and E_h are the electric field components with vertical and horizontal polarizations, respectively, and η is the electromagnetic wave impedance of the medium.

[37] In polarimetric remote sensing radiometry, the Stokes parameters are conventionally expressed in terms of brightness temperature:

$$\begin{aligned} T_I &= T_{vv} + T_{hh} = \frac{\lambda^2}{k_B B} I, \\ T_Q &= T_{vv} - T_{hh} = \frac{\lambda^2}{k_B B} Q, \\ T_U &= T_{45} + T_{-45} = \frac{\lambda^2}{k_B B} U, \\ T_V &= T_{\mathrm{lc}} + T_{\mathrm{rc}} = \frac{\lambda^2}{k_B B} V, \end{aligned} \tag{A2}$$

where λ is the wavelength of the wave, k_B is the Boltzmann's constant, and B is the noise-equivalent bandwidth. T_{vv} and T_{hh} are the vertical and horizontal brightness temperatures, T_{45} and T_{-45} represent orthogonal measurements skewed 45° with respect to normal, and T_{lc} and T_{rc} refer to left-hand and right-hand circular polarized quantities. Note that in previously published literature, I, Q, U, and V have also been used for the Stokes parameters in brightness temperature, instead of T_I, T_Q, T_U, and T_V, which was a source of confusion. This practice was agreed to be discouraged by *Randa et al.* [2008].

[38] Generally, the energy emitted from the Earth's surface is partly polarized, meaning that the vertical brightness temperature is different from the horizontal. Whereas conventional dual-polarization radiometers only measure vertical and horizontal polarized brightness temperatures, a polarimetric radiometer is capable of directly or indirectly measuring all four Stokes parameters, which provides a full characterization of the polarization properties of the emitted energy. In remote sensing, third and fourth Stokes parameters are primarily used for correcting polarization rotations, or, for instance, in the case of the ocean, to infer wind direction information.

[39] **Acknowledgments.** The work presented in this paper was supported by the Spanish Ministry of Science and Education under the FPU grant AP2003-4912 and projects ESP2007-65667-C04-02 and AYA2008-05906-C02-01/ESP. The SMOS-BEC is a joint initiative of CSIC and UPC mainly funded by the Spanish Ministry of Education and Science through the National Program on Space.

References

Camps, A., M. Vall.llossera, N. Duffo, F. Torres, and I. Corbella (2005), Performance of sea surface salinity and soil moisture retrieval algorithms with different auxiliary datasets in 2-D L-band aperture synthesis interferometric radiometers, *IEEE Trans. Geosci. Remote Sens.*, *43*, 1189–1200.

Choudhury, B., T. Schmugge, A. Chang, and R. Newton (1979), Effect of surface roughness on the microwave emission from soils, *J. Geophys. Res.*, *84*, 5699–5706.

Davenport, I. J., J. Fernandez-Galvez, and R. J. Gurney (2005), A sensitivity analysis of soil moisture retrieval from the tau-omega microwave emission model, *IEEE Trans. Geosci. Remote Sens.*, *43*, 1304–1316.

Dobson, M. C., F. T. Ulaby, M. T. Hallikainen, and M. A. El-Rayes (1985), Microwave dielectric behavior of wet soil—Part II: Dielectric mixing models, *IEEE Trans. Geosci. Remote Sens.*, *23*, 35–46.

Entekhabi, D., et al. (1999), An agenda for land surface hydrology research and a call for the Second International Hydrological Decade, *Bull. Am. Meteorol. Soc.*, *80*, 2043–2058.

Escorihuela, M., Y. Kerr, P. de Rosnay, J. P. Wigneron, J. Calvet, and F. Lemaitre (2007), A simple model of the bare soil microwave emission at L-band, *IEEE Trans. Geosci. Remote Sens.*, *45*, 1978–1987.

European Space Agency (2003), Mission objectives and scientific requirements of the SMOS mission, version 5, technical report, Paris. (Available at http://www.cesbio.ups-tlse.fr/)

European Space Agency (2006), SEPS architectural detailed design document, *Tech. Rep. ADDD V5.0*, Paris. (Available at http://cassiopea.estec.esa.int/SEPS/Documents/)

European Space Agency (2007), Algorithm Theoretical Bases Document, *Tech. Rep. 3.a*, Paris. (Available at http://www.cesbio.ups-tlse.fr/)

Hornbuckle, B. K., and A. W. England (2005), Diurnal variation of vertical temperature gradients within a field of maize: Implications for satellite microwave radiometry, *IEEE Geosci. Remote Sens. Lett.*, *2*, 74–77.

Hornbuckle, B. K., A. W. England, R. D. de Roo, M. A. Fischman, and D. L. Boprie (2003), Vegetation canopy anisotropy at 1.4 GHz, *IEEE Trans. Geosci. Remote Sens.*, *41*, 2211–2222.

Jackson, T. J., and T. J. Schmugge (1989), Passive microwave remote sensing system for soil moisture: Some supporting research, *IEEE Trans. Geosci. Remote Sens.*, *27*, 225–235.

Jackson, T. J., et al. (1999), Soil moisture mapping at regional scales using microwave radiometry: The southern Great Plains hydrology experiment, *IEEE Trans. Geosci. Remote Sens.*, *37*, 2136–2151.

Kerr, Y., P. Waldteufel, J. P. Wigneron, J. Font, and M. Berger (2001), Soil moisture retrieval from space: The soil moisture and ocean salinity (SMOS) mission, *IEEE Trans. Geosci. Remote Sens.*, *39*, 1729–1735.

Kirdiashev, K. P., A. A. Chukhantsev, and A. M. Shutko (1979), Microwave radiation of the Earth's surface in presence of vegetation cover, *Radio Eng. Electron.*, *24*, 256–264.

Krajewski, W., et al. (2006), A remote sensing observatory for hydrologic sciences: A genesis for scaling to continental hydrology, *Water Resour. Res.*, *42*, W07301, doi:10.1029/2005WR004435.

Marquardt, D. (1963), An algorithm for least-squares estimation of nonlinear parameters, *J. Soc. Ind. Appl. Math.*, *11*, 431–441.

Martín-Neira, M., S. Ribó, and A. J. Martín-Polegre (2002), Polarimetric mode of MIRAS, *IEEE Trans. Geosci. Remote Sens.*, *40*, 1755–1768.

Meesters, A., R. de Jeu, and M. Owe (2005), Analytical derivation of the vegetation optical depth from the microwave polarization difference index, *IEEE Geosci. Remote Sens.*, *2*, 121–123.

Mo, T., B. Choudhury, T. Schmugge, and T. Jackson (1982), A model for microwave emission from vegetation-covered fields, *J. Hydrol.*, *184*, 101–129.

Monerris, A. (2009), Experimental estimation of soil emissivity and its application to soil moisture retrieval in the SMOS mission, Ph.D. thesis, Univ. Politec. de Catalunya, Barcelona, Spain. (Available at http://www.tesisenxarxa.net/TDX-1228109-101841/)

National Research Council (2007), *Earth Science and Applications From Space: National Imperatives for the Next Decade and Beyond*, Space

Stud. Board, Natl. Acad., Washington, D. C. (Available at http://www.nap.edu)

Njoku, E., and D. Entekhabi (1996), Passive microwave remote sensing of soil moisture, *J. Hydrol.*, *184*, 101–129.

Owe, M., R. de Jeu, and J. P. Walker (2001), A methodology for surface soil moisture and vegetation optical depth retrieval using the microwave polarization difference index, *IEEE Trans. Geosci. Remote Sens.*, *39*, 1643–1654.

Pardé, M., J. P. Wigneron, P. Waldteufel, Y. Kerr, A. Chanzy, S. S. Sobjaerg, and N. Skou (2004), N-parameter retrievals from L-band microwave observations acquired over a variety of crop fields, *IEEE Trans. Geosci. Remote Sens.*, *42*, 1168–1178.

Pellarin, T., J. P. Wigneron, J. Calvet, and P. Waldteufel (2003), Global soil moisture retrieval on a synthetic L-band brightness temperature data set, *J. Geophys. Res.*, *108*(D12), 4364, doi:10.1029/2002JD003086.

Randa, J., et al. (2008), Recommended terminology for microwave radiometry, technical report, Natl. Inst. of Stand. and Technol., Gaithersburg, Md. (Available at http://www.grss-ieee.org/education/standard-terminology/)

Sabia, R., A. Camps, M. Talone, M. Vall-llossera, and J. Font (2010), Determination of sea surface salinity error budget in the soil moisture and ocean salinity mission, *IEEE Trans. Geosci. Remote Sens.*, in press.

Saleh, K., et al. (2009), Soil moisture retrievals at L-band using a two-step inversion approach (COSMOS/NAFE'05 Experiment), *Remote Sens. Environ.*, *113*, 1304–1312.

Schmugge, T., W. Kustas, J. Ritchie, T. Jackson, and A. Rango (2002), Remote sensing in hydrology, *Adv. Water Resour.*, *25*, 1367–1385.

Schneeberger, K., M. Schwank, C. Stamm, P. de Rosnay, C. Mätzler, and H. Flühler (2004), Topsoil structure influencing soil water retrieval by microwave radiometry, *Vadose Zone J.*, *3*, 1169–1179.

Talone, M., A. Camps, B. Mourre, R. Sabia, M. Vall-llossera, J. Gourrion, C. Gabarró, and J. Font (2009), Simulated SMOS levels 2 and 3 products: The effect of introducing ARGO data in the processing chain and its impact on the error induced by the vicinity of the coast, *IEEE Trans. Geosci. Remote Sens.*, *47*, 3041–3050.

Ulaby, F. T., and A. E. Wilson (1985), Microwave attenuation properties of vegetation canopies, *IEEE Trans. Geosci. Remote Sens.*, *23*, 746–753.

Ulaby, F., R. Moore, and A. Fung (1981), *Microwave Remote Sensing: Active and Passive*, Artech House, Norwood, Mass.

van de Griend, A., and J. P. Wigneron (2004), The b-factor as a function of frequency and canopy type at H-polarization, *IEEE Trans. Geosci. Remote Sens.*, *42*, 786–794.

Vine, D. L., and S. Abraham (2002), The effect of the ionosphere on remote sensing of the sea surface salinity from space: Absorption and emission at L-band, *IEEE Trans. Geosci. Remote Sens.*, *40*, 771–782.

Wagner, W., G. Blsch, P. Pampaloni, J. Calvet, B. Bizarri, J. P. Wigneron, and Y. Kerr (2007), Operational readiness of microwave remote sensing of soil moisture for hydrologic applications, *Nordic Hydrol.*, *38*, 1–20.

Waldteufel, P., and G. Caudal (2002), About off-axis radiometric polarimetric measurements, *IEEE Trans. Geosci. Remote Sens.*, *40*, 1435–1439.

Wan, Z. (2008), New refinements and validation of the MODIS land-surface temperature/emissivity products, *Remote Sens. Environ.*, *112*, 59–74.

Wang, J., and B. Choudhury (1981), Remote sensing of soil moisture content over bare field at 1.4 GHz frequency, *J. Geophys. Res.*, *86*, 5277–5282.

Wang, J. R., and T. J. Schmugge (1980), An empirical model for the complex dielectric permittivity of soils as a function of water content, *IEEE Trans. Geosci. Remote Sens.*, *18*, 288–295.

Wigneron, J. P., A. Chanzy, J. Calvet, and N. Bruguier (1995), A simple algorithm to retrieve soil moisture and vegetation biomass using passive microwave measurements over crop fields, *Remote Sens. Environ.*, *51*, 331–341.

Wigneron, J. P., P. Waldteufel, A. Chanzy, J. Calvet, and Y. Kerr (2000), Two-dimensional microwave interferometer retrieval capabilities over land surfaces (SMOS-mission), *Remote Sens. Environ.*, *73*, 270–282.

Wigneron, J. P., L. Laguerre, and Y. Kerr (2001), A simple parameterization of the L-band microwave emission from rough agricultural soils, *IEEE Trans. Geosci. Remote Sens.*, *39*, 1696–1707.

Wigneron, J., et al. (2007), L-Band Microwave Emission of the Biosphere (L-MEB) Model: Description and calibration against experimental data sets over crop fields, *Remote Sens. Environ.*, *107*, 639–655.

A. Camps, A. Monerris, M. Piles, M. Talone, and M. Vall-llossera, Remote Sensing Laboratory, Departament de Teoria del Senyal i Comunicacions, Universitat Politècnica de Catalunya, c/Jordi Girona 1-3, E-08034 Barcelona, Spain. (maria.piles@tsc.upc.edu)

J. M. Sabater, European Centre for Medium-Range Weather Forecasts, Shinfield Park, Reading RG2 9AX, UK.